



## MATHEMATICAL MODELING OF AN AVALANCHE RELEASE AND ESTIMATION OF FLOW PARAMETERS

MAHMOUD ZARRINI<sup>1\*</sup> AND R. N. PRALHAD<sup>2</sup>

<sup>1</sup>Department of Applied Mathematics, University of Ayatollah Boroujerdi, Boroujerd, Iran.

<sup>2</sup>Department of Mathematics, Defence Institute of Advanced Technology, Pune, India.

### AUTHORS' CONTRIBUTIONS

This work was carried out in collaboration between both authors. Both authors read and approved the final manuscript.

*Received: 12 August 2021*

*Accepted: 25 October 2021*

*Published: 29 October 2021*

*Original Research Article*

### ABSTRACT

In this paper, estimation of velocity, maximum velocity, dynamic pressure of snow avalanche release and Run-out zone distance over mountain regions are studied. To investigate of mathematical model, we have been taken gravitational, turbulent and friction forces with momentum equation. Computation of flow parameters such as velocity (both in start to track zone and from track to run out zone), maximum velocity (in track zone) and dynamic pressure and estimation of run out distance have been calculated. The flow parameters have been computed for its variation with slope angle, frictional coefficient, eddy viscosity, and different flow heights.

**Keywords:** Avalanche velocity; dynamic pressure; run-out distance; snow avalanche.

**MSC Numbers:** 47N40, 34-XX.

### 1. INTRODUCTION

One of the serious threats for the people living in snow bound hilly regions is an avalanche wherein there is loss of property and at times loss of lives if one gets caught in it [1, 2]. Though advent of science has helped in estimating the danger associated with it however triggering of an avalanche could not be predict well in advance due to complex nature of snow and its behavior with the surroundings. The cause of an avalanche is basically associated with instability in the snow pack [3,4,5,6]. This instability is developed as a result of metamorphism in snow pack due to temperature gradient resulting in

developing depth hoar crystals near the ground which are very fragile in nature and any extra weight (as a result of walking or addition precipitation of snow on this snow pack) will make the entire snow pack to slide down. There are other factors which can contribute to the avalanche such as temperature metamorphism, pressure metamorphism and wind induced drift activity [7,8,9]. Many authors have proposed models on avalanche dynamics and estimated values for velocity at starting and track [1, 10-14]. In view of its importance in the cold science, study pertaining to an avalanche, estimation of the flow parameters pertaining to an avalanche has been initiated in the present model.

\*Corresponding author: Email: dr\_mzarrini@yahoo.com;

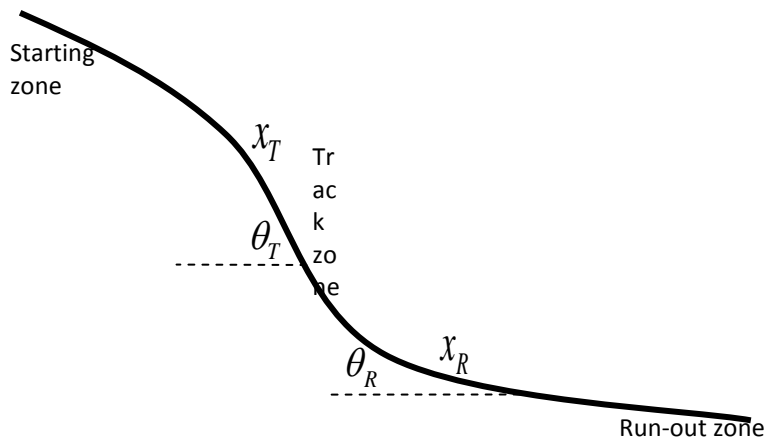


Fig. 1. Three stages of an avalanche release

2. ANALYSIS

In order to estimate velocity, maximum velocity and run-out zone distance of an avalanche release, we consider the snow movement down the hill in three different zones (starting zone, track zone and run-out zone) (Fig. 1) by following assumptions :

- (i) Flow is steady
- (ii) Flow is one dimensional,
- (iii) Flow is without any stress force

Momentum equation can be written as [15]:

$$\rho V \frac{dV}{dt} = f_g - f_f - f_t \tag{1}$$

Where  $V$  is avalanche velocity,  $\rho$  is snow density,  $f_g$  is gravitational force,  $f_f$  is friction force and  $f_t$  is turbulent force (Fig. 2)

$$f_g - f_f - f_t = \rho g (\sin \theta - \mu_f \cos \theta) - \frac{\rho g}{R \eta^*} V^2 \tag{2}$$

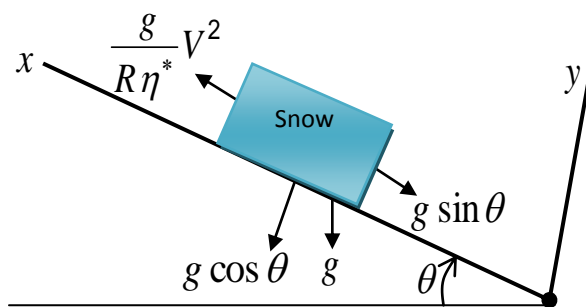


Fig. 2. Body force representation on a slab

Where  $\eta^*$  is eddy viscosity and  $R$  is  $\frac{BH}{2H+B}$  since  $H \ll B$  then  $R$  (slab depth) is approximated to  $H$  ( $R \approx H$ ) (Fig. 3).

Equation (1) simplifies to:

$$\frac{dV^2}{dx} = 2g (\sin \theta(x) - \mu_f \cos \theta(x)) - \frac{2g}{\eta^* H} V^2 \tag{3}$$

Where,  $\theta(x)$  is slope angle at position  $x$  along incline,  $g$  is acceleration due to gravity and  $\mu_f$  is a constant coefficient of sliding friction.

It is assumed that in segment start to track zone length is  $x_T$  and slope angle is  $\theta_T$ , and avalanche accelerates here. Similarly in track to run-out zone,  $x_R$  is run out distance,  $\theta_R$  is the slope angle and avalanche decelerates here.

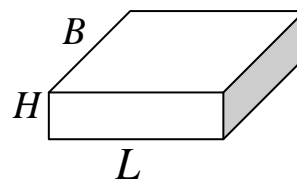


Fig. 3. Snow slab dimension

### 2.1 Avalanche Velocity from Start to Track Zone

In start zone to track zone, the solution of equation (3) with  $\theta(x) = \theta_T$  is given by

$$V(x) = \sqrt{C_T \exp\left(-\frac{2gx}{\eta^* H}\right) + \eta^* H (\sin \theta_T - \mu_f \cos \theta_T)} \tag{4}$$

Where  $C_T$  is a constant and it determined with initial condition in start zone  $V(0) = 0$  as:

$$C_T = -\eta^* H (\sin \theta_T - \mu_f \cos \theta_T) \tag{5}$$

Then, velocity between start zone to track zone is

$$V(x) = \sqrt{\eta^* H (\sin \theta_T - \mu_f \cos \theta_T) \left(1 - \exp\left(-\frac{2gx}{\eta^* H}\right)\right)} \tag{6}$$

Maximum velocity in track zone can be estimated by the assumption that

$$1 - \exp\left(-\frac{2gx}{\eta^* H}\right) \ll 1 \tag{7}$$

Then, equation (6) becomes:

$$V(x_T) \approx V_{Max} = \sqrt{\eta^* H (\sin \theta_T - \mu_f \cos \theta_T)} \tag{8}$$

### 2.2 Avalanche Velocity from Track to Run-out Zone

Avalanche velocity between track zone and run out zone is obtained by assuming initial velocity in track zone is maximum velocity and solving the differential equation (3) with  $\theta(x) = \theta_R$  as:

$$V(x) = \sqrt{C_R \exp\left(-\frac{2gx}{\eta^* H}\right) - \eta^* H (\mu_f \cos \theta_R - \sin \theta_R)} \tag{9}$$

Using the initial condition  $V(0) = V_{Max}$ , when  $x = 0$ , Equation (9) yields

$$V(x) = \sqrt{V_{Max}^2 \exp\left(-\frac{2gx}{\eta^* H}\right) + \eta^* H (\mu_f \cos \theta_R - \sin \theta_R) \left[\exp\left(-\frac{2gx}{\eta^* H}\right) - 1\right]} \tag{10}$$

In addition,  $\mu_f$  is greater than zero, as required for flowing avalanches, and the condition  $\frac{dV}{dx} \leq 0$  must

be applied at the beginning to the avalanche decelerates in this region on the lower slope. The range of  $\mu_f$  can be estimated by using Equation (10)

$$\text{and } \frac{dV}{dx} \leq 0 \tag{11}$$

$$\tan \theta_R \leq \mu_f \leq \tan\left(\frac{\theta_T + \theta_R}{2}\right)$$

The data required for the computation is taken from [7,10-14,4] are tabulated in Table 1.

### 2.3 Run-out Distance

Run out distance  $x_R$  can be estimated by assuming that  $V(x_R) = 0$  to equation (10) and run out distance can be obtained by approximating the relation by the Maclaurin's series and neglecting second and higher order terms in it.

$$\exp\left(-\frac{2gx_R}{\eta^* H}\right) \approx 1 - \frac{2gx_R}{\eta^* H} \tag{Assumption:}$$

$$\frac{1}{2} \left(\frac{2gx_R}{\eta^* H}\right)^2 \ll 1 \tag{12}$$

Table 1. Data of flow parameters

Symbol	Description	Typical value	Range
$\theta_T$	Slope angle at Track zone	38°	30 – 45
$\theta_R$	Slope angle at Run-out zone	9°	0 – 11
$\eta^*$	Eddy viscosity	600 m/s <sup>2</sup>	400 – 1200
$H$	Slab height	1.5 m	1 – 2
$\rho$	Snow density	200 kg/m <sup>3</sup>	100 – 300
$x_T$	Distance Start zone to Track zone	100 m	50 – 200
$\mu_f$	Coefficient of sliding friction	0.3 kg/m.s	0.158– 0.531

Approximated run out distance can be estimated to:

$$x_R(Approx) = \frac{V_{Max}^2}{2g(\mu_f \cos \theta_R - \sin \theta_R + \frac{V_{Max}^2}{\eta^* H})} \quad (13)$$

Equation (10) may be compared to the approximate run-out equation given by Voellmy [15] with the modification suggested by Salm [13]

$$x_R(Salm) = \frac{V_{Max}^2}{2g(\mu_f \cos \theta_R - \tan \theta_R + \frac{V_{Max}^2}{2\eta^* H})} \quad (14)$$

Exact run out distance can be estimated by making  $V(x_R) = 0$  in equation (10):

$$x_R(Exact) = \frac{\eta^* H}{2g} \ln \left( \frac{V_{Max}^2 + \eta^* H (\mu_f \cos \theta_R - \sin \theta_R)}{\eta^* H (\mu_f \cos \theta_R - \sin \theta_R)} \right) \quad (15)$$

### 3. RESULTS AND DISCUSSION

Computation of velocity from start to track zone has been estimated by using equation (6). Variation has been observed for different flow parameters [coefficient of friction ( $\mu_f$ ), slope angle ( $\theta_T$ ), slab depth ( $H$ ) and eddy viscosity ( $\eta^*$ )]. The results have been shown in Figs. 4–7.

The results indicate that, velocity increases with increase in slab depth ( $H$ ), slope angle ( $\theta_T$ ), eddy

viscosity ( $\eta^*$ ) and decrease in friction coefficient ( $\mu_f$ ). Maximum velocity has been computed by using Equation (8). Computation of maximum velocity for different flow parameters has been tabulated in Table 2 and the range of maximum velocity by this method is almost between 14 m/s to 23 m/s. The computed results [Figs. 4–7 and Table 2] have been found to agree well with the physical observations since velocity to increase with increase in slab depth ( $H$ ), slope angle ( $\theta_T$ ), eddy viscosity ( $\eta^*$ ) and with decrease in friction coefficient ( $\mu_f$ ).

Computation of velocity between track and run out zone is done by using equation (10). The computed values are shown in Figs. 8–14. The range of  $\mu_f$  has been computed by using equation (11) and data from Table 1 and equation (12). The results of velocity in track to run out zone again found to be in similar variations with the one observed in the start to track zone by approximation method [Figs. 8–13]. Also avalanche velocity between track and run out zone has been computed by using Equation (10). It is observed that the velocity decreases to zero to the estimated run out zone [Fig. 14].

Estimation of run out distance has been done by both methods; one approximating by Maclaurin’s series [equation (13)] and Salm [13] method [equation (14)] another one by exact approach [equation (15)]. The details of computation are shown in Table 3. The results indicate that, the variation in exact to approximation method is between 29 to 82% and by exact to Salm (1979) method is between 7 to 64%.

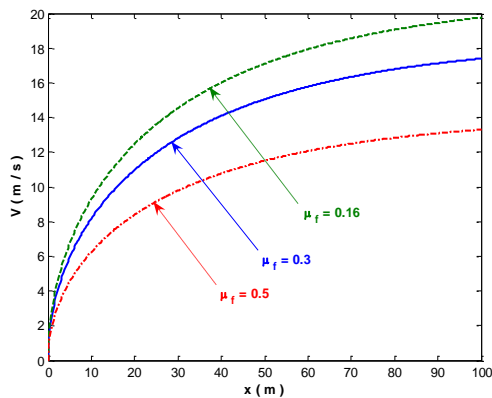


Fig. 4. Variation of velocity with distance (start to track zone) for different friction coefficients ( $\mu_f$ )

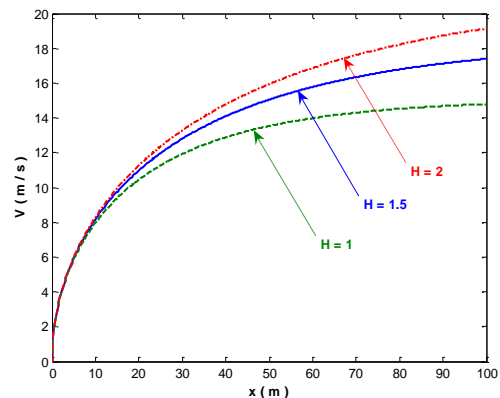


Fig. 5. Variation of velocity with distance (start to track zone) for different slab depth ( $H$ )

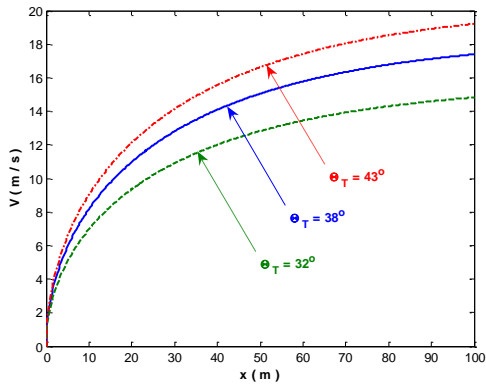


Fig. 6. Variation of velocity with distance (start to track zone) for different slope angle ( $\theta_T$ )

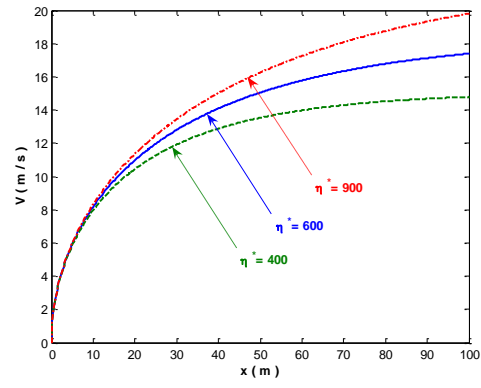


Fig. 7. Variation of velocity with distance (start to track zone) for different eddy viscosity ( $\eta^*$ )

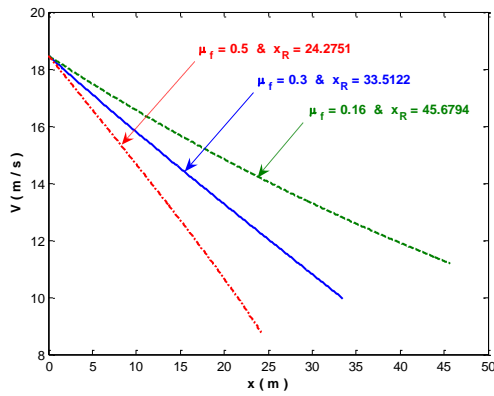


Fig. 8. Variation of velocity with distance (track to run-out zone) for different  $\mu_f$  and  $x_R$

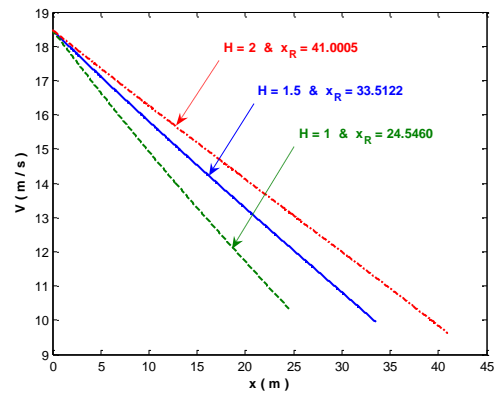


Fig. 9. Variation of velocity with distance (track to run-out zone) for different  $H$  and  $x_R$

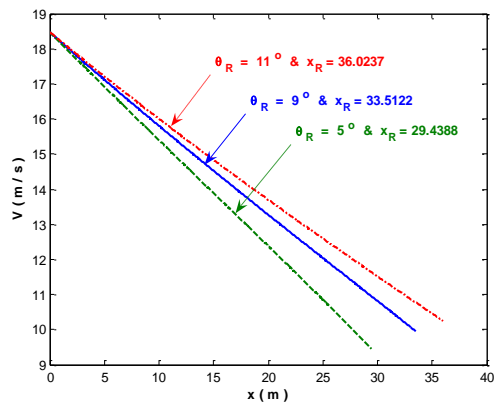


Fig. 10. Variation of velocity with distance (track to run-out zone) for different  $\theta_R$  and  $x_R$

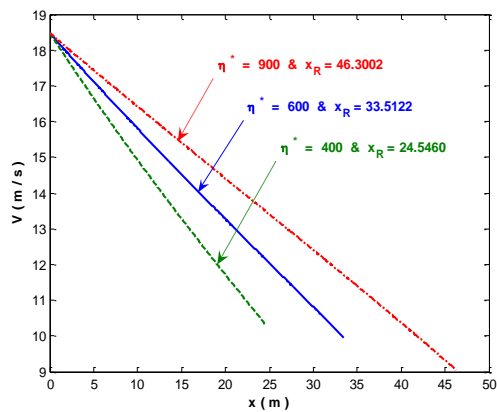


Fig. 11. Variation of velocity with distance (track to run-out zone) for different  $\eta^*$  and  $x_R$

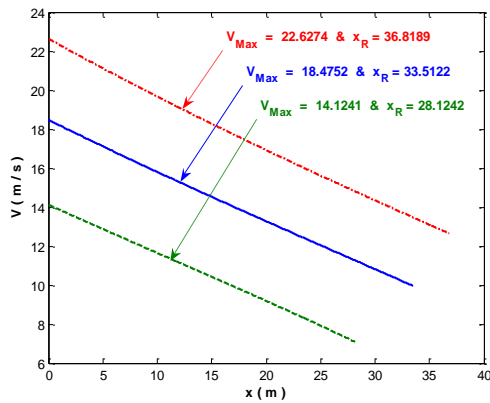


Fig. 12. Variation of velocity with distance (track to run-out zone) for different  $V_{Max}$  and  $x_R$

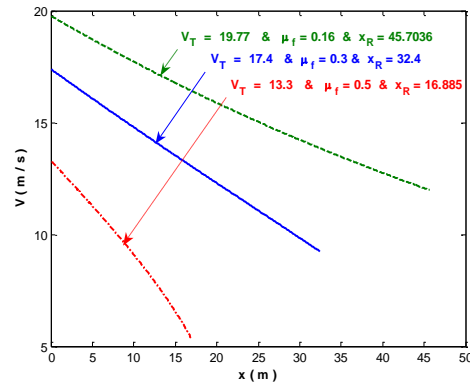


Fig. 13. Variation of velocity with distance (track to run-out zone) for different  $V_T$ ,  $\mu_f$  and  $x_R$

Table 2. Computation of maximum velocity for different flow parameters

$\theta_T$	$\eta^*$	$\mu_f$	$H$	$V_{Max}$
38	600	0.16	1.5	20.9910
38	600	0.3	1.5	18.4752
38	600	0.5	1.5	14.1241
38	600	0.3	1	15.0849
38	600	0.3	2	21.3333
32	600	0.3	1.5	15.7466
43	600	0.3	1.5	20.4042
38	400	0.3	1.5	15.0849
38	900	0.3	1.5	22.6274

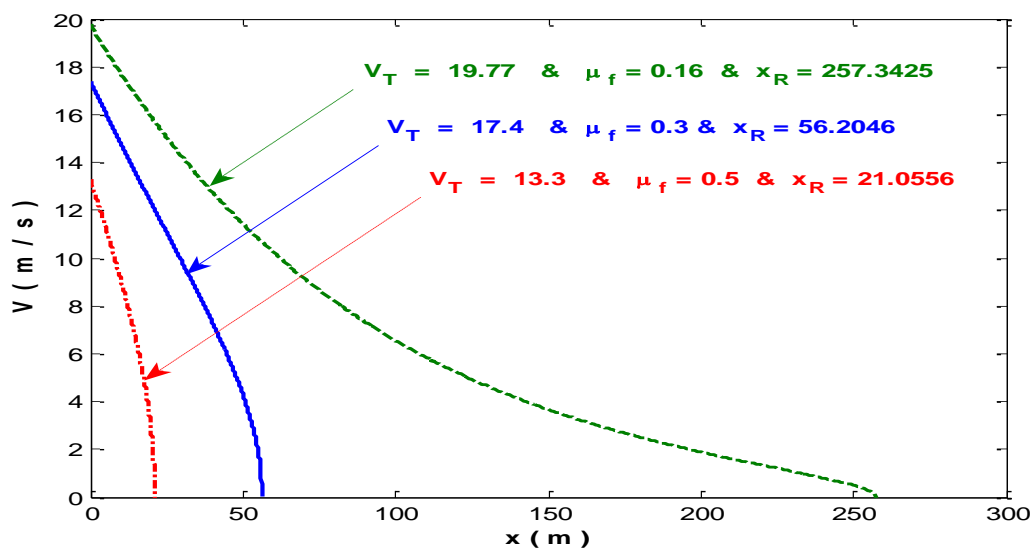
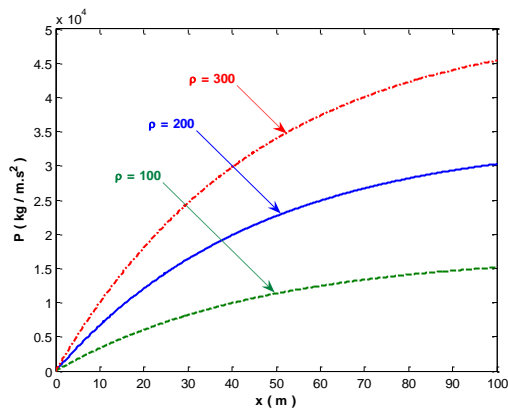


Fig. 14. Variation of velocity with distance (track to run-out zone) for different  $V_T$ ,  $\mu_f$  and run out distance ( $x_R$ ) [Exact approach (equation 13)]

**Table 3. Computation of run out distance for both approximate [equations (13), (14)] and Exact [equation (15)] methods for different flow parameters**

$\theta_R$	$\eta^*$	$\mu_f$	$H$	$V_{Max}$	$x_R$ App.	$x_R$ Salm	$x_R$ Exact	Error % App.	Error % Salm
9	600	0.16	1.5	18.4752	45.6794	90.9776	251.1525	81.8121	63.7760
9	600	0.3	1.5	18.4752	33.5122	52.7985	60.1573	44.2924	12.2326
9	600	0.5	1.5	18.4752	24.2751	33.0093	34.5558	29.7510	4.4754
9	600	0.3	1	18.4752	24.5460	41.0005	49.6266	50.5386	17.3820
9	600	0.3	2	18.4752	41.0005	61.6716	67.8747	39.5938	9.1390
5	600	0.3	1.5	18.4752	29.4388	43.3486	47.0903	37.4844	7.9458
11	600	0.3	1.5	18.4752	36.0237	59.3136	70.5774	48.9586	15.9595
9	400	0.3	1.5	18.4752	24.5460	41.0005	49.6266	50.5386	17.3820
9	900	0.3	1.5	18.4752	46.3002	65.3314	71.0330	34.8187	8.0267
9	600	0.3	1.5	14.1241	28.1242	40.5572	43.5601	35.4359	6.8937
9	600	0.3	1.5	22.6274	36.8189	61.5008	74.4399	50.5388	17.3819



**Fig. 15. Variation of dynamic pressure with distance (start to track zone) for different snow density**

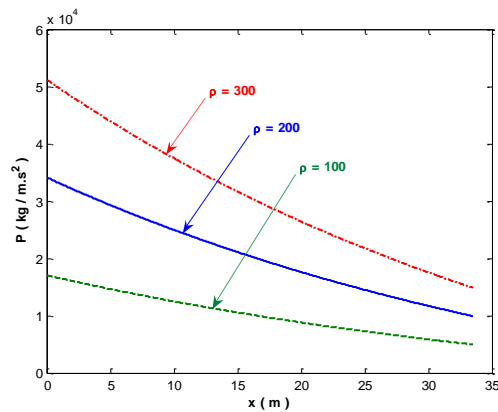


**Fig. 16. Variation of dynamic pressure with distance (track to run-out zone) for different snow density**

**4. AVALANCHE DYNAMIC PRESSURE**

Dynamic pressure has been computed by the relation (given by White, [16])

$$p = \frac{1}{2} \rho V^2 \tag{16}$$

for both start to track zone and track to run-out zone. The computed results have been shown in Fig. 15. The variation has been observed with different snow densities.

It is observed that, dynamic pressure increases with increase in snow density and track distance in start to track zone [Fig. 15]. Whereas it is observed to decrease with decrease in snow density and increase in run-out distance [Fig. 16].

**5. CONCLUSIONS**

The results indicate that, velocity of snow avalanche (in start zone to track zone) increases with increase in

distance ( $x$ ), height of snow over the hill ( $H$ ), slope angle ( $\theta$ ), eddy viscosity ( $\eta^*$ ) and decreasing frictional coefficient ( $\mu_f$ ).

Velocity of snow avalanche between track zone and run out zone is found to decrease as reaches the ground location. These observations are found to be in agreement with the physics of flow and deformation of snow. The results of the present investigations can be used for the design of control structures for the mitigational aspect of avalanches.

**COMPETING INTERESTS**

Authors have declared that no competing interests exist.

**REFERENCES**

1. Atwater MM, Kozoil FC. Avalanche Handbook, USDA forest service; 1952.

2. Saller R, et al. Snow avalanche mass-balance calculation and simulation-model verification, *Annals of Glaciology*. 2008;48.
3. Bader H, Kuroiwa D. The physics and mechanics of snow as a material. CRREL monograph, part II, section B; 1962.
4. Zarrini M, Pralhad RN. Estimation of vapor velocity, vapor density and vapor temperature in a snow pack and its application in avalanche forecasting, *Journal of Heat and Mass Transfer*. 2012;55(19):4965-4969.
5. Zarrini M. Mathematical modeling of snow drifts transport by wind over the mountain terrain, *Journal of Hyperstructures*. 2013; 2(2):201–206.
6. Blagovechshenskiy V, Eglit M, Naaim M. The calibration of an avalanche mathematical model using field data, *Natural Hazards and Earth System Sciences*. 2002;2:217–220.
7. Mellor M. Engineering properties of snow. *Journal of Glaciology*; 1977.
8. Colbeck SC. Thermodynamics of snow metamorphism due to variations in curvature, *Journal of Glaciology*; 1980.
9. Yosida Z. Physical properties of snow, *Ice and snow Properties, Processes, and Applications*, The M.I.T. Press, Cambridge, MA, W.D. Kingery, editor; 1963.
10. Bartelt P, Salm B, Gruber U. Calculating dense-snow avalanche run-out using a Voellmy-fluid model with active/passive longitudinal straining. *Journal of Glaciology*. 1999;45(150):242–254.
11. McClung DM. Derivation of Voellmy's maximum speed and run-out estimates from a center-of-mass model, *Journal of Glaciology*. 1983;29(102).
12. Perla RI, Cheng TT, McClung DM. A two-parameter model of snow-avalanche motion. *Journal of Glaciology*. 1980;26(94):197–207.
13. Salm B. On non-uniform , steady flow of avalanching snow. IASH Publisher. 1986;79:161–188.
14. Schweizer J. Review of dry snow slab avalanche release. *Cold Region Science and Technology*. 1999;30: 43–57.
15. Voellmy A. On the destructive force of avalanches. *Alta avalanche study Center, Transl*. 1966;2:63.
16. White FM. *Fluid mechanics*, Mc-Graw-Hill; 2003.